Eur. Phys. J. B **9**, 323–333 (1999)

THE EUROPEAN PHYSICAL JOURNAL B

EDP Sciences

Theoretical description of adatom migration in two-dimensional highly-ordered states

A.A. Chumak[1] and C. Uebing[2,3,a]

[1] Institute of Physics of the National Academy of Sciences, pr. Nauki 46, 252028, Kiev, Ukraine
[2] Max-Planck-Institut für Eisenforschung, 40074 Düsseldorf, Germany
[3] Lehrstuhl für Physikalische Chemie II, Universität Dortmund, 44227 Dortmund, Germany

Received 24 June 1998

Abstract. Analytical expressions for chemical, jump, and tracer diffusion coefficients are obtained for interacting lattice gases on a square lattice. Strongly repulsive nearest neighbor interactions cause the formation of a highly-ordered c(2×2) state in the vicinity of half coverage. It is shown that only strongly correlated successive adatom jumps contribute to the particle flow. This allows to describe the adatom kinetics by considering an almost ideal lattice gas of defects. Two types of defects are considered, adatoms in the empty sublattice and vacancies in the filled sublattice of the c(2×2) ordered state. The diffusion equations for these defects are developed considering the generation and recombination of defects. In addition we have considered adatom transport caused by the motion of defect pairs (dimers). Dimer transport mechanism prevails in the high coverage region. The characteristic features of the various diffusion coefficients near half coverage are analyzed and discussed. The theory is compared with the results of sophisticated Monte-Carlo simulations which have been executed with the use of a fully parallelized algorithm on a Cray T3E (LC784-128). The agreement between theoretical and MC results is excellent if the motion of dimers at $\theta > 0.5$ is taken into account.

PACS. 82.20.Mj Nonequilibrium kinetics – 68.35.Fx Diffusion; interface formation – 64.60.Cn Order-disorder transformations; statistical mechanics of model systems

1 Introduction

The chemical diffusion coefficient $D_{\rm c}$ of a non-interacting lattice gas is independent of coverage in the absence of adatom-adatom interaction. It is well-known that repulsive adatom-adatom interactions result in an increase of $D_{\rm c}$. Even in the absence of macroscopic concentration gradients local (*i.e.* microscopic) coverage inhomogeneities might exist, which induce local forces causing the relaxation to the uniform state. These local forces can be seen to some respect as an thermodynamic force $\partial\mu/\partial\mathbf{r}$ (here μ is the chemical potential of the adatom system) which causes local adatom flows like an external field.

This idea has been confirmed by analytic calculations (see *e.g.* [1]) and Monte-Carlo (MC) simulation [2]. Progresses in the theoretical description of low-dimensional systems made it possible to calculate diffusion coefficients for a one-dimensional chain with nearest neighbor (NN) interactions [3] and to study the adatom migration in the vicinity of the order-disorder phase transition [4–6]. The main result of [4,5] is that the coverage dependence of diffusion is non-monotonous in narrow regions near the order-disorder phase transition points and for half coverage. This remarkable result was confirmed using the real space renormalization group (RSRG) approach [6,7].

Extensive MC simulations [8] using powerful computer algorithms have revealed the most obvious peculiarities of the adatom diffusion for the simplest two-dimensional systems (square lattice, NN interactions). At finite surface coverages tracer (D^*) and jump diffusion coefficient ($D_{\rm j}$) behave remarkably different compared to the chemical diffusion coefficient (see [1,8] for definitions of these quantities). For the non-interacting case $D_{\rm j}$ and $D_{\rm c}$ are simply related *via* [9]

$$D_{\rm c} = \frac{D_{\rm j}}{1-\langle n\rangle}\,. \tag{1}$$

Here $\langle n\rangle \equiv \theta$ is the mean value of the lattice site occupation number, which corresponds to the surface coverage θ. In the presence of adatom-adatom interactions this simple relationship is no longer valid.

Long-range correlations constitute the main difficulty in the analytical investigation of lattice gas properties. The correlation length (i) increases as a lattice gas system approaches an order-disorder phase transition, and (ii) diminishes both in the well-ordered and disordered states. Nevertheless, there is an essential difference in the description of adatom migration in ordered and disordered states.

[a] e-mail: uebing@mpie-duesseldorf.mpg.de

The transition of the system into an ordered state lowers its symmetry. In order to describe an adatom system, one needs to know, along with the coverage, at least one more physical quantity (for example, the order parameter). Therefore, the adatom migration in general depends on the dynamics of several physical quantities.

In this work we study the adatom migration on a square lattice taking strongly repulsive NN interactions $\varphi \gg 1$ into account. Here φ represents the NN interaction energy in units of kT. At temperatures below T_c [10] these interactions cause c(2×2) ordering of the adatoms. We will restrict the considerations to a small range of coverages $\theta \approx 0.5$ at temperatures $T < T_c$. Sharply at half coverage, $\theta = 0.5$, the lattice gas shows the most ordered c(2×2) structure with a very short correlation length. Under such circumstances the lattice is divided into two sublattices of filled and empty sites. At finite temperatures below T_c there are defects in both sublattices (occupied sites in the empty sublattice, which in the following will be denoted black defects, and vacancies in the filled sublattice, white defects). If the density of these defects is very small, *i.e.* for $|\theta - 0.5| \equiv |\delta| \to 0$ and $\varphi \gg 1$, it should be possible to treat them as an ideal gas. Random adatom jumps may cause the annihilation of different defects (recombination) and the thermal generation of defect pairs as well. The equilibrium concentration of defects can be obtained both from the generation-recombination (GR) balance condition and in terms of thermodynamic considerations. The main idea of the paper is to describe the adatom migration by considering the motion of the two different defects in the approximation of an (almost) ideal lattice gas scheme.

Based on this approach (Sect. 2) we will calculate diffusion coefficients (Sects. 3–5) and compare them with the results of sophisticated Monte-Carlo simulations (Sect. 6) which are executed using a fully parallelized algorithm on the Cray T3E (LC672-128) operated by the Max-Planck community in Garching/Germany. Details of the Monte-Carlo procedure are given in [11] and will be briefly described in Section 6.

2 Thermodynamics of defects

In thermodynamic equilibrium the adatom system is described by the statistical operator ρ,

$$\rho = Q^{-1} \exp\left[\sum_i \mu n_i - \varphi \sum_{(i,j)} n_i n_j\right]. \tag{2}$$

Here the first sum runs over all lattice sites i, while the second one runs over all pairs of NN sites (i,j). $n_{i,j}$ describes the local occupancy number,

$$n_i = \begin{cases} 1, \text{ if site } i \text{ is occupied} \\ 0, \text{ if site } i \text{ is vacant.} \end{cases} \tag{3}$$

The partition function Q is given by

$$Q = \sum_{\{n_i\}} \exp\left[\sum \mu n_i - \varphi \sum n_i n_j\right]. \tag{4}$$

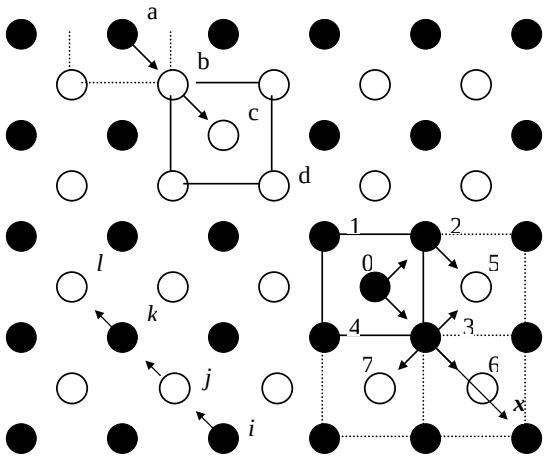

Fig. 1. Square lattice of adsorption sites. At low temperatures the lattice can be divided into two interpenetrating sublattices of empty (black circles) and filled sites (open circles). Empty sites of the filled sublattice form white defects, while filled sites of the empty sublattice form black defects.

At low temperatures the lattice can be divided into two interpenetrating sublattices of empty and filled sites in such a way that the NN sites of a given filled site belong to the empty sublattice, and *vice versa* (Fig. 1). The summation over the variables of a given sublattice can be carried out explicitly. In the following we will describe this procedure for the empty sublattice:

$$\begin{aligned} Q &= \prod_i \sum_{\{n_i\}} \sum_{\{n_j\}} \exp\left\{ n_i \left(\mu - \varphi \sum_j n_j \right) + \frac{\mu}{4} \sum_j n_j \right\} \\ &\equiv \prod_i \sum_{\{n_j\}} \exp\left(\frac{\mu}{4} \sum_j n_j \right) \left[1 + \exp\left(\mu - \varphi \sum n_j \right) \right]. \end{aligned} \tag{5}$$

Here the index j runs over the NN sites of a given site i. The most probable values of $\sum_j n_j$ are 4 and 3 (the probability that two or more defects are present as nearest neighbors of site i is negligibly small when $\varphi \gg 1$ and $|\theta - 0.5| \to 0$), as already mentioned. Under this assumption the last term of equation (5) can be transformed as

$$1 + \exp\left(\mu - \varphi \sum n_j \right) = C \exp\left(\sum \frac{\mu' - \mu}{4} n_j \right). \tag{6}$$

The two constants C and μ' can be written as

$$\begin{aligned} C &= \left(1 + \mathrm{e}^{\mu - 3\varphi}\right)^4 \left(1 + \mathrm{e}^{\mu - 4\varphi}\right)^{-3} \\ \mathrm{e}^{\mu'} &= \mathrm{e}^{\mu} \frac{\left(1 + \mathrm{e}^{\mu - 4\varphi}\right)}{C}. \end{aligned} \tag{7}$$

With equations (5, 6) the partition function can be written as

$$Q = \left[C \left(1 + \mathrm{e}^{\mu'} \right) \right]^{N/2}. \tag{8}$$

Here N is the total number of lattice sites. The chemical potential μ and the surface coverage θ are related by the thermodynamic equation $\theta = (\partial \ln Q/\partial\mu)/N$. In the limiting case $e^{\mu-3\varphi} \ll 1$, the following explicit formula can be given,

$$e^{\mu-4\varphi} \cong \delta + \left(\delta^2 + e^{-4\varphi}\right)^{1/2}. \quad (9)$$

This equation can also be obtained in a similar way for the other sublattice (with i sites belonging to the filled sublattice). However, the criterion $e^{\mu-3\varphi} \ll 1$ must be replaced by $e^{\mu-\varphi} \gg 1$. It is interesting to note that the condition $e^{\mu-\varphi} \gg 1$ implies that $-\delta e^{\varphi} \ll 1$ for $\delta < 0$. The condition $e^{\mu-3\varphi} \ll 1$ means that $\delta e^{\varphi} \ll 1$ for $\delta > 0$.

It follows from equation (9) that the chemical potential is equal to 2φ at half coverage, *i.e.* for $\delta = 0$. This statement can be proved independently by considering the symmetry of the system as the variables n_i are replaced by $(1 - n_i)$ (particle-hole symmetry).

It is straightforward to show that $e^{\mu-4\varphi} \equiv n^{\mathrm{b}}$ is equal to the mean value of $|n_i n_j|$ (where i and j denote NN sites). $|n_i n_j|$ is the probability to find an adatom in the empty lattice (see Fig. 1, the black defect at site 0). $e^{-\mu} \equiv n^{\mathrm{w}}$ is the probability to find a vacancy in the filled lattice (see Fig. 1, the white defect at site c). It follows from equation (9) that $n^{\mathrm{w}} < n^{\mathrm{b}}$ if $\theta > 0.5$, and $n^{\mathrm{w}} > n^{\mathrm{b}}$ if $\theta < 0.5$. The product of the probabilities n^{b} and n^{w} does not depend on θ,

$$n^{\mathrm{b}} n^{\mathrm{w}} = e^{-4\varphi} = const. \quad (10)$$

This relation is very important for the understanding of peculiar features of the adatom transport. It shows that the minimum total number of mass carriers $(n^{\mathrm{b}} + n^{\mathrm{w}})N/2$ is present at $\theta = 0.5$. In the following sections we shall see that both tracer and jump diffusion coefficients show deep minima close to half coverage.

The dependence $\mu(\theta)$ is very steep, *i.e.* one can considerably change the value of μ by slight changes of θ. The derivative $\partial\mu/\partial\theta = (\delta^2 + e^{-4\varphi})^{-1/2}$ has a sharp maximum for $\delta = 0$. We shall see in the following sections that the competition of the thermodynamic factor $(\theta\partial\mu/\partial\theta)$ and the mass carrier concentrations (n^{b} and n^{w}) determines the behavior of the chemical diffusion coefficient in the vicinity of $\theta = 0.5$.

3 Migration of defects: jump and tracer diffusion coefficients

In this section we will describe the motion of defects. Our considerations are based on the rate equation for the adatom motion

$$\frac{n_i(t + \Delta t) - n_i(t)}{\Delta t} = \sum_k \left[\nu_{ki} n_k (1 - n_i) - \nu_{ik} n_i (1 - n_k)\right] \quad (11)$$

in the limit $\Delta t \to 0$. Equation (11) describes changes of the local occupation numbers n_i due to adatom jumps to empty (or from filled) NN sites (index k). The probability of an adatom jump ν_{ki} depends on the interaction with adatoms on NN sites. As in previous work [8] we assume

$$\nu_{kl} = \nu_\circ \exp\left[\varepsilon_k\right] \quad (12)$$

where $\nu_\circ = const.$ ε_k is the total interaction energy of the moving adatom on its initial site k and its nearest neighbors.

Our purpose is to study the black defect migration in terms of equations (11, 12) only. Figure 1 shows that the black defect at site 0 can move to an adjacent vacant site of the empty sublattice by means of two successive adatom jumps. In order to move the black defect from site 0 to site 6 it is necessary (i) that the adatom on site 3 jumps to site 6 and (ii) that the adatom on site 0 jumps to site 3. In principle it is also possible that the adatom on site 6 jumps back to site 3 in step ii (backward jump). It follows from equation (12) that the probability of the first jump $(3 \to 6)$ is equal to $\nu_\circ e^{\varphi}$. The probability of the second jump $(0 \to 3)$ (and also of the backward jump $6 \to 3$) is equal to $\nu_\circ e^{3\varphi}$. This value is by the factor $e^{2\varphi}$ greater than that of the first jump $(3 \to 6)$. Hence, the total probability of the defect transition for a short time interval Δt is determined by the probability of the first adatom jump only. With Δt chosen in the interval

$$\nu_\circ e^{\varphi} \ll \Delta t^{-1} \ll \nu_\circ e^{3\varphi} \quad (13)$$

the probability of the defect jump $(0 \to 6)$ in time Δt is equal to

$$\Delta t \frac{1}{2} \nu_\circ e^{\varphi} \equiv \Delta t \gamma_\varphi. \quad (14)$$

Here γ_φ denotes the jump frequency of black defects. Thus, the defect transition from site 0 to site 6 may be regarded as a single jump in the time scale determined by equation (13). This jump event consists of two strongly correlated successive adatom jumps, where the second jump immediately follows the first one. The probability of the $0 \to 6$ transition can be obtained more rigorously by integrating the kinetic equation (Eq. (11)) over the time interval defined by equation (13). The initial conditions for the variables n_i must be taken in accordance with the configuration depicted in Figure 1.

The above consideration yields the jump frequency of black defects to the next nearest site (NNN) of the empty sublattice to be equal to γ_φ. The jumps of black defect to NN sites of the same sublattice (for example, $0 \to 5$) occur with probabilities by the factor of two higher because there are two symmetric passes ($0 \to 2 \to 5$ and $0 \to 3 \to 5$) which contribute to the total probability. The free motion of black defects is governed by the rate equation similar to equation (11), *i.e.*

$$\frac{n_i^{\mathrm{b}}(t + \Delta t) - n_i^{\mathrm{b}}(t)}{\Delta t} = 2\gamma_\varphi \sum_{\mathrm{NN}} \left\{n_k^{\mathrm{b}} - n_i^{\mathrm{b}}\right\} + \gamma_\varphi \sum_{\mathrm{NNN}} \left\{n_k^{\mathrm{b}} - n_i^{\mathrm{b}}\right\} \quad (15)$$

where the sums run over NN and NNN of site i. Equation (15) which describes the uncorrelated jumps of black defects is linear with respect to n_i^{b}.

The rate equation for white defects can be obtained in a very similar way. The resulting rate equation

$$\frac{n_i^{\mathrm{w}}(t+\Delta t)-n_i^{\mathrm{w}}(t)}{\Delta t} = 2\gamma \sum_{\mathrm{NN}} \{n_k^{\mathrm{w}} - n_i^{\mathrm{w}}\} + \gamma \sum_{\mathrm{NNN}} \{n_k^{\mathrm{w}} - n_i^{\mathrm{w}}\} \qquad (16)$$

reproduces the form of equation (15) but contains the jump probability γ, which is determined by

$$\gamma \equiv \frac{1}{2}\nu_\circ \ll \gamma_\varphi. \qquad (17)$$

Figure 1 allows to explain this difference. It is evident that the jump of a white defect from site c to site a is performed by means of two successive adatom jumps, $a \to b$ and $b \to c$. The first jump is not activated in contrast to the case of black defect motion.

It is straightforward to extend the theory to the case of adatom motion in a weak uniform field $\mathbf{E}$ with the adatom-field interaction term being defined as $H_E = -\mathbf{E}\sum_i \mathbf{r}_i$. Here $\mathbf{r}_i$ is the position of the ith adatom. The barrier heights are lowered by the value $Ea/2$ for the adatom motion in the direction of the field and are increased by the same value for the opposite jumps. In the presence of a field the probabilities of defect jumps are also changed with regard for the adatom ones. A simple analysis shows that the changes of the jump probabilities are given by

$$\gamma_\varphi \to \begin{cases} \gamma_\varphi(1+Ea), & \text{for } 0 \to 6, \\ \gamma_\varphi(1+Ea/4), & \text{for } 0 \to 3 \to 5, \\ \gamma_\varphi(1+3Ea/4), & \text{for } 0 \to 2 \to 5. \end{cases} \qquad (18)$$

Here we assume that $\mathbf{E}$ lies in the x direction (*i.e.* along $0 \to 6$ in Fig. 1). The other probabilities are easily determined by a symmetry analysis. Employing the modified defect jump probabilities, we obtain the contribution of the black defect motion for the adatom flow density,

$$j^{\mathrm{b}} = 4\gamma_\varphi n^{\mathrm{b}} E. \qquad (19)$$

The white defect motion gives a similar contribution. Thus, the total density of the adatom flow is given by

$$j = 4(\gamma_\varphi n^{\mathrm{b}} + \gamma n^{\mathrm{w}})E. \qquad (20)$$

The effective conductivity $\sigma = 4(\gamma_\varphi n^{\mathrm{b}} + \gamma n^{\mathrm{w}})$ of the adatom system can be expressed as product of the adatom concentration

$$c = (\theta/a^2) \approx 1/(2a^2) \qquad (21)$$

and the mobility b, *i.e.* $\sigma = bc$. Thus, the adatom mobility (which by definition corresponds to the jump diffusion coefficient D_{j}) is given by

$$b \equiv D_{\mathrm{j}} = 8a^2(\gamma_\varphi n^{\mathrm{b}} + \gamma n^{\mathrm{w}}) \equiv 4D_\circ(\mathrm{e}^{\varphi} n^{\mathrm{b}} + n^{\mathrm{w}}). \qquad (22)$$

Here $D_\circ = \nu_\circ a^2$ is the chemical diffusion coefficient of adatoms in the absence of adatom-adatom interactions. It is possible to interpret the quantities $4D_\circ \mathrm{e}^{\varphi}$ and $4D_\circ$ as mobilities (or jump diffusion coefficients) of black and white defects, respectively. It follows from equation (22) that D_{j} depends on the numbers of black *and* white defects. One has to expect that D_{j} is small in the coverage range where the numbers of mass carriers are small (*i.e.* in the vicinity of half coverage, see Sect. 2). The minimum of D_{j} must occur slightly below $\theta = 0.5$ due to factor e^{φ} within the brackets of equation (22). With equation (9) we obtain the explicit form of D_{j} as

$$D_{\mathrm{j}} = 4D_\circ \left[(\mathrm{e}^{\varphi}-1)\delta + (\mathrm{e}^{\varphi}+1)\sqrt{\delta^2 + \mathrm{e}^{-4\varphi}}\right] \qquad (23)$$

In Section 5 we give a more detailed analysis of the dependencies of D_{j} on θ and φ.

A similar procedure can be employed in order to obtain the tracer diffusion coefficient. Let us consider an adatom system that is a mixture of ordinary and tagged particles (tracers). The tracer concentration c^* is negligibly small, and the tracer interaction parameter is similar to that of ordinary particles. Thus, there is no space-time correlation of different tagged particles. The tracer diffusion coefficient D^* describes the motion of individual particles (single particle diffusion coefficient) in contrast to the chemical and jump diffusion coefficients (many particle diffusion coefficients). In order to calculate the tracer diffusion coefficient we shall first obtain the tracer conductivity σ^*.

The flow of tracers in an external field is also associated with defect motion. However, only jumps of tagged particles contribute. For the situation depicted in Figure 1 the following jumps contribute to the tracer flow in $+x$ direction: (i) $0 \to 2 \to 5$ if site 2 is occupied by a tracer; (ii) $0 \to 3 \to 5$ if site 0 is occupied by a tracer; and (iii) $0 \to 3 \to 6$ if the sites 0 or 3 are occupied by tracers. The case (iii) requires some comments. The probability of both jumping adatoms (on sites 0 and 3) to be tagged is negligible. Thus, the contribution of black defect jumps to NNN sites to the mobility of tracers is half compared to the mobility of ordinary particles. Straightforward calculations similar to those used to obtain equation (20) yield the tracer conductivity, which is given by

$$\sigma^* = 4D_\circ \left(\frac{3}{4}\mathrm{e}^{\varphi} n^{\mathrm{b}} + n^{\mathrm{w}}\right) c^*. \qquad (24)$$

As previously, the coefficient in front of c^* in equation (24) means tracer mobility which for the case of small tracer concentration is tracer diffusion coefficient D^* too. The last statement can be easily proved by straightforward calculations of the value of the tracer flow caused by small gradient of c^*. Hence, the tracer diffusion coefficient has the form

$$D^* = 4D_\circ \left(\frac{3}{4}\mathrm{e}^{\varphi} n^{\mathrm{b}} + n^{\mathrm{w}}\right). \qquad (25)$$

The first and the second term in the brackets of equation (25) are associated with the motion of black and

white defects, respectively. One can easily see the broken symmetry in the contribution of black and white defects to D^* (factor 3/4). This factor accounts for the difference between D^* and the jump diffusion coefficient D_j of ordinary adatoms (see Eq. (22)). In order to explain this peculiarity we recall that there is a certain difference in the transport of black and white defects. The transport of a black defect to a NNN site involves the jump of only *one tagged* particle over a distance a. In contrast, the transport of a white defect may involve the displacement of a tagged particle over a distance $2a$ (in case of $a \to b \to c$, Fig. 1). The physical reason of this phenomena is that the transport of white defects requires two successive jumps of the same adatom, while the transport of black defects requires jumps of two different adatoms. It is important to note that there is no such asymmetry with respect to the transport of ordinary particles. In this case, the transport of a black defect to a NNN site displaces two particles to the distance a. This situation is fully equivalent to the displacement of one particle to the distance $2a$ which occurs during the transport of a white defect.

It should be noted here that the concept of defect migration was employed in [12,13] to explain the peculiarities of lattice-gas diffusion which have been revealed under MC simulation in the vicinity of stoichiometric concentrations. Kutner, Binder and Kehr (see [12]) studied diffusion in face-centered-cubic lattice gas with repulsive NN interaction but with particle jump mechanism different from ours (determined by Eq. (12)). The explicit term responsible for vacancy jump probability was found in [12]. Similarly to our case, it was considered the two-step jump mechanism with the first step being rate-limiting in low-temperature range. The vacancy jump probability was found to be two times higher than the probability of the first step or equal to it (see in [12] Eqs. (6, 7) respectively). It contradicts with equation (17) of the present paper which shows that on the average only half of the first-step successful events results in the vacancy transitions. Nevertheless, both approaches give similar qualitative description of the vacancy jump.

4 Chemical diffusion coefficient

The linear equation (15) can be used to find the chemical diffusion coefficient of black defects, D^b. If we assume that the black defect concentration n^b smoothly varies in space one can expand the quantities in the right-hand part of equation (15) in a series of small jump distances $\mathbf{a}_j$:

$$n^\mathrm{b}(\mathbf{r}_i) - n^\mathrm{b}(\mathbf{r}_j) = n^\mathrm{b}(\mathbf{r}_i) - n^\mathrm{b}(\mathbf{r}_i + \mathbf{a}_j). \qquad (26)$$

Figure 1 shows that $|\mathbf{a}_j| = \sqrt{2}a$ for jumps to NN sites (or $|\mathbf{a}_j| = 2a$ for jumps to NNN sites). Thus, the diffusion coefficient of black defects is equal to $D^\mathrm{b} = 4D_\circ \mathrm{e}^{\varphi}$. A similar procedure gives the diffusion coefficient of white defects to be equal to $D^\mathrm{w} = 4D_\circ$. It is interesting to note that D^b and D^w reproduce the mobilities (or jump diffusion coefficients) of black and white defects obtained in Section 3. The diffusion equations for both species are given by

$$\frac{\partial n^\mathrm{b}}{\partial t}(\mathbf{r},t) = D^\mathrm{b}\Delta n^\mathrm{b}(\mathbf{r},t),$$
$$\frac{\partial n^\mathrm{w}}{\partial t}(\mathbf{r},t) = D^\mathrm{w}\Delta n^\mathrm{w}(\mathbf{r},t). \qquad (27)$$

Equation (27) describes the evolution of an ideal gas of defects which depends on the initial and boundary conditions. On the other hand, to describe the evolution of long-scale inhomogeneities with the characteristic length of the order of or greater than the mean interdefect distance one has to account for generation-recombination (GR) processes as already discussed in Section 1. For this purpose, we have to add GR terms in the right-hand parts of equation (27).

The recombination term R has the form $R = -\sum_j \Gamma_{ij} n_i^\mathrm{b} n_j^\mathrm{w}$, where Γ_{ij} is of the order of γ_φ and $|\mathbf{r}_i - \mathbf{r}_j| = 3a, \sqrt{5}a$. To comprehend the microscopic recombination mechanism, we have to consider the situation depicted in Figure 1, where the black and white defects in the sites 0 and c can recombine with probability $2\gamma_\varphi$ (for unit time). It is just the probability of an adatom to jump from site 1 to site d. A relatively insignificant time is taken then for completing the recombination act by means of the adatom jumps ($0 \to 1$ and $d \to c$). The exact values of Γ_{ij} can be easily obtained in a similar fashion to γ_φ (see Sect. 3), but their explicit form is irrelevant for the following analysis.

The generation term can be obtained by analogy with γ_φ. To create one pair (black and white defects), three successive adatom jumps have to be undertaken. Detailed description of generation mechanism is given in Appendix A.

Introducing both G and R terms in the right-hand parts of equation (27) yields a system of interconnected equations

$$\frac{\partial n^\mathrm{b}}{\partial t}(\mathbf{r},t) = D^\mathrm{b}\Delta n^\mathrm{b}(\mathbf{r},t) + G - R,$$
$$\frac{\partial n^\mathrm{w}}{\partial t}(\mathbf{r},t) = D^\mathrm{w}\Delta n^\mathrm{w}(\mathbf{r},t) + G - R. \qquad (28)$$

In the equilibrium state the derivatives in equation (28) are equal to zero, and both equations reduce to the evident condition $G = R$ which determines the product of the mean defect concentrations

$$n^\mathrm{b} n^\mathrm{w} = \frac{G}{\Gamma} = const\, \exp(-4\varphi), \qquad (29)$$

where $\Gamma = \sum_j \Gamma_{ij} = 28\nu_\circ \mathrm{e}^{\varphi}$, and $G = 28\nu_\circ \mathrm{e}^{-3\varphi}$ (see Appendix A), $const = 1$. We have already derived this relation in Section 2 (see Eq. (10)) on pure thermodynamic grounds.

If the defect concentrations slightly differ from their equilibrium values ($n_i^\mathrm{b} - n^\mathrm{b} \equiv \delta n_i^\mathrm{b} \ll n^\mathrm{b}$, $n_i^\mathrm{w} - n^\mathrm{w} \equiv \delta n_i^\mathrm{w} \ll n^\mathrm{w}$) then one can linearize the GR term with respect to δn^b and δn^w:

$$G - R \approx \Gamma(\delta n_i^\mathrm{b} n^\mathrm{w} + \delta n_i^\mathrm{w} n^\mathrm{b}). \qquad (30)$$

Equation (30) can be used to transform equation (28) to a system of linear equations which describe the effect of (i) diffusion and (ii) GR processes on the evolution of coupled disturbances $\delta n_i^{\rm b}$ and $\delta n_i^{\rm w}$. Once $\delta n^{\rm b}$ and $\delta n^{\rm w}$ are known, we can easily obtain the adatom density disturbance $\delta c = (\delta n^{\rm b} - \delta n^{\rm w})/(2a^2)$.

It is important to distinguish two different regimes of the coverage inhomogeneity relaxation, *i.e.*,

$$\begin{aligned} &\text{(i)} \quad D^{\rm b,w} l^{-2} \gg \Gamma n^{\rm b,w}, \\ &\text{(ii)} \quad D^{\rm b,w} l^{-2} \ll \Gamma n^{\rm b,w}, \end{aligned} \tag{31}$$

where l is the characteristic inhomogeneity length. Case (i) describes diffusive flows of both species when the influence of the GR processes is negligible. The diffusional decay of coverage inhomogeneities includes two stages. The first one is due to fast diffusion of black defects, and the second one is due to the (slow) diffusion of white defects. The rigorous description of the coverage evolution for this case is possible only if the initial profiles and boundary conditions for black and white defects are known. This observation is very important to design reliable computer simulations, especially when the number of lattice sites is not too high. One can see that the Boltzmann-Matano scheme is not appropriate for obtaining the adatom diffusion coefficient in this particular case since two different diffusion coefficients are involved in the adatom transport.

Case (ii) describes also a two-stage evolution process. After the first (fast) stage, the local equilibrium is established with $\delta n^{\rm b} n^{\rm w} = -\delta n^{\rm w} n^{\rm b}$. This means that the quantities $\delta n^{\rm b,w}$ are determined by the disturbance of the chemical potential only. The last statement can be proved with the use of the explicit forms of $n^{\rm b}$ and $n^{\rm w}$ (see Sect. 2). Considering the local equilibrium condition and equation (28), we derive the following diffusion equation for adatom migration,

$$\frac{\partial c}{\partial t}(\mathbf{r}, t) = D_{\rm c} \Delta c(\mathbf{r}, t), \tag{32}$$

where $D_{\rm c}$ is the chemical diffusion coefficient determined by $D_{\rm c} = (D^{\rm b} n^{\rm b} + D^{\rm w} n^{\rm w})/(n^{\rm b} + n^{\rm w})$. Using equation (9) and the relations $n^{\rm b} = \exp(\mu - 4\varphi)$ and $n^{\rm w} = \exp(-\mu)$ we find that

$$n^{\rm b} + n^{\rm w} = 2\sqrt{\delta^2 + {\rm e}^{-4\varphi}} = (\partial \mu / \partial \ln \theta)^{-1} \tag{33}$$

and $D_{\rm c} = (\partial \mu / \partial \ln \theta)(D^{\rm b} n^{\rm b} + D^{\rm w} n^{\rm w}) = (\partial \mu / \partial \ln \theta) D_{\rm j}$, where $D_{\rm j}$ is just the jump diffusion coefficient obtained in Section 3 for the adatom transport in an external field E (see Eq. (22)). With regard for equation (9) the explicit form of $D_{\rm c}$ is given by

$$D_{\rm c} = 2D_\circ \left[1 + {\rm e}^{\varphi} + ({\rm e}^{\varphi} - 1)\delta(\delta^2 + {\rm e}^{-4\varphi})^{-1/2}\right]. \tag{34}$$

The diffusion coefficient $D_{\rm c} = (\partial \mu / \partial \ln \theta) D_{\rm j}$ describes the local equilibrium regime of adatom diffusion. Our approach deals with the kinetics of black and white defects only. However, it is the generation-recombination processes which establishes the local equilibrium state in the defect system. Therefore, it is possible to conclude that $D_{\rm c}$ describes the GR-controlled stage of the decay of coverage inhomogeneities. The local value of the chemical potential is the only physical quantity that determines the smoothly in space and time varying defect concentrations at this stage.

In conclusion of this Section, it should be noted that the explicit form of $D_{\rm c}$ (see Eq. (34)) can be obtained employing a thermodynamic term (see Eq. (9) and the last paragraph of Sect. 2) and a mobility term (Eq. (22)). However, our analysis gives the possibility to describe adatom migration beyond the local equilibrium state (using Eq. (28)) and to find the explicit criteria of the local equilibrium regime of diffusion (see Eq. (31), case (ii)).

5 The dimer motion effect on the diffusion coefficients

In the preceding Section 3, the jump diffusion coefficients were derived as linear forms of the defect concentrations $n^{\rm b}$ and $n^{\rm w}$. The reason for this procedure was our assumption that δ is the small parameter of the theory. In this case, the total number of defects $n^{\rm b} + n^{\rm w}$ is limited by the greater of the numbers $2|\delta|$ and $2{\rm e}^{-2\varphi}$, and is minimal when $\delta = 0$. On the other hand, the contribution of black defects is determined by the factor $n^{\rm b}{\rm e}^{\varphi}$. In contrast to $n^{\rm b}$, this factor can be much larger than one, *i.e.* $n^{\rm b}{\rm e}^{\varphi} \gg 1$ for $\delta \neq 0$ and $\varphi \gg 1$. Thus quadratic elements in $n^{\rm b}{\rm e}^{\varphi}$ terms could give the dominant contribution in $D_{\rm j}$, D^* and $D_{\rm c}$. Let us consider the situation that two black defects forming a NN dimer are placed in the neighboring sites (0 and 5) of the empty sublattice (see Fig. 1). The probabilities of adatom jumps from sites 2 or 3 are by the factor ${\rm e}^{\varphi}$ higher than in the case of an isolated defect. This first adatom jump is immediately followed by a second jump. After this series of jump events the NN dimer is transformed either into a similar NN or into a NNN dimer. Very similar conclusions can be given if we consider the situation that two black defects are placed in NNN sites (*e.g.* sites 0 and 6) of the empty sublattice. Therefore, we can regard the black dimers as long-living objects (on the time scale $(\nu_\circ {\rm e}^{2\varphi})^{-1}$), which perform many jumps before disintegration. This physical picture is in accordance with our theoretical analysis in [14] where the effective attraction of NN and NNN black defects was found.

In the following we shall investigate the contribution of pairs of black defects (black dimers) on the adatom transport. We will start with the calculation of the total number of dimers, $N_{\rm d}^{\rm b}$, which is given by

$$N_{\rm d}^{\rm b} \equiv N_{\rm NN}^{\rm b} + N_{\rm NNN}^{\rm b} = 2N(n^{\rm b})^2 = n^{\rm b} 8 n^{\rm b} \frac{N}{2} \frac{1}{2} \cdot \tag{35}$$

Here $N_{\rm NN}^{\rm b}$ and $N_{\rm NNN}^{\rm b}$ are the average numbers of dimers formed by NN and NNN black defects, respectively. In order to illustrate equation (35) we note that the total number of dimers depends (1) on the probability to find an isolated defect in each site of the sublattice ($n^{\rm b}$), (2) the

average number of NN and NNN defects for such an isolated defect ($8n^{\mathrm{b}}$) and (3) the total number of sublattice sites ($N/2$). The factor $1/2$ avoids the double counting of dimers. The relative contribution of black dimers to the black defect transport is of the order of $n^{\mathrm{b}}\mathrm{e}^{\varphi}$.

Detailed calculations (see Appendix B) show that the increase of jump diffusion coefficient due to black dimer motion is determined by

$$\Delta D_{\mathrm{j}} = \frac{16}{3} D_{\circ} \mathrm{e}^{2\varphi} (n^{\mathrm{b}})^2. \tag{36}$$

Comparing equation (36) with equation (22) shows that ΔD_{j} constitutes the dominant contribution in the D_{j} when $\theta - 0.5 \geq (3/8)\mathrm{e}^{-\varphi}$. The effect of black dimers is negligible for coverages $\theta < 0.5$.

In principle, also white dimers (*i.e.* dimers formed by NN or NNN white defects) should be considered. Quadratic terms in n^{w} are much less significant compared to quadratic terms in $n^{\mathrm{b}}\mathrm{e}^{\varphi}$ (by a factor of $\mathrm{e}^{2\varphi}$). The contribution of white dimer motion can be obtained formally from equation (36) by substitution of 1 for $\mathrm{e}^{2\varphi}$, and n^{w} for n^{b}. At the same time, we must take into account the effective decrease of the number of isolated white defects. Detailed analysis shows the negative contribution of white dimer configurations in jump diffusion coefficient. It is determined by

$$\Delta D_{\mathrm{j}} = -\frac{20}{3} D_{\circ} (n^{\mathrm{w}})^2. \tag{37}$$

White dimers reduce adatom mobility, in contrast to black dimers. However, as already mentioned their influence could be small.

For the sake of simplicity, the theoretical results for the adatom mobilities were derived so far from conductivity terms in which the quantity $1/2a^2$ was substituted for the exact value of the adatom density $c = \theta/a^2$ (Eq. (21)). Thus, we have to multiply the theoretical results for the adatom mobilities by the factor of $(2\theta)^{-1}$, and the definitive expression for the jump diffusion coefficient is

$$D_{\mathrm{j}} = \frac{2}{\theta} D_{\circ} \times \Bigg[\underbrace{\mathrm{e}^{\varphi} n^{\mathrm{b}}}_{\text{black defects}} + \underbrace{n^{\mathrm{w}}}_{\text{white defects}} + \underbrace{\frac{4}{3}\mathrm{e}^{2\varphi}(n^{\mathrm{b}})^2}_{\text{black dimers}} - \underbrace{\frac{5}{3}(n^{\mathrm{w}})^2}_{\text{white dimers}} \Bigg]. \tag{38}$$

The dimer contribution in the tracer diffusion coefficient can be determined in a quite similar fashion by using the jump probabilities in an external field. Omitting the details of the calculations, we present the definitive form of D^* as follows

$$D^* = \frac{2}{\theta} D_{\circ} \times \Bigg[\underbrace{\frac{3}{4}\mathrm{e}^{\varphi} n^{\mathrm{b}}}_{\text{black defects}} + \underbrace{n^{\mathrm{w}}}_{\text{white defects}} + \underbrace{\mathrm{e}^{2\varphi}(n^{\mathrm{b}})^2}_{\text{black dimers}} - \underbrace{\frac{5}{3}(n^{\mathrm{w}})^2}_{\text{white dimers}} \Bigg]. \tag{39}$$

Comparison of equations (38, 39) shows that the influence of black dimers on D^* is by the factor of $3/4$ lower compared to D_{j}. The reason for the asymmetry of black and white defects contribution in D^* and D_{j} was explained in Section 3: only one tagged particle can be displaced to the distance a during the single defect jump.

6 Comparison of theoretical results and Monte-Carlo simulations

In the previous sections we have obtained various diffusion coefficients considering a linear response of the system to an external field or concentration gradient. The obtained kinetic coefficients describe dissipative processes and are related to the corresponding equilibrium time correlation functions *via* the fluctuation-dissipation theorem. In particular, the conductivity of the system σ can be expressed in terms of a current-current correlator according to

$$\sigma = bc = \frac{1}{4Na^2} \int_{-\infty}^{+\infty} \mathrm{d}t \langle \mathbf{v}_i(t)\, \mathbf{v}_k(0) \rangle. \tag{40}$$

Here $\mathbf{v}_i$ is the velocity of the ith adatom. The correlator in the right side of equation (40) can be rewritten in terms of mean square displacements. It follows from equation (40) that

$$b = D_{\mathrm{j}} = \lim_{t\to\infty} \frac{1}{4tN_{\mathrm{a}}} \left\langle \Big[\sum_i \Delta\mathbf{r}_i(t) \Big]^2 \right\rangle. \tag{41}$$

Here $\Delta\mathbf{r}_i(t)$ is the displacement of the ith adatom at time t, N_{a} is the total number of adatoms.

The expression for tracer mobility (tracer diffusion coefficient) can be easily obtained from equation (41) in a rather formal way by substituting the total number of tracers N^* for N_{a} and neglecting the correlation of different tagged particles (rarefied gas of tracers). Thus, in accordance with [1] we can write

$$D^* = \lim_{t\to\infty} \frac{1}{4tN^*} \sum_i \langle [\Delta\mathbf{r}_i(t)]^2 \rangle. \tag{42}$$

In the state of local equilibrium, the chemical diffusion coefficient D_{c} can be expressed *via* D_{j} and the thermodynamic factor as [15]

$$D_{\mathrm{c}} = \left(\frac{\partial\mu}{\partial \ln\theta} \right)_T D_{\mathrm{j}} = \left[\frac{\langle (\delta N)^2 \rangle}{\langle N \rangle} \right]^{-1} D_{\mathrm{j}}. \tag{43}$$

Here $\langle (\delta N)^2 \rangle$ is the mean square number fluctuation in an area A containing on average $\langle N \rangle$ particles.

Our Monte-Carlo simulation of tracer and jump diffusion coefficients employs just the expressions (41, 42). These quantities are determined from the measurements of both mean-square displacements of N^* tagged adatoms (see Eq. (42)), and the center of mass mean-square displacements (see Eq. (41)). We applied a sophisticated Monte-Carlo algorithm to simulate particle motion in initially fully equilibrated adsorbate layers (for details see

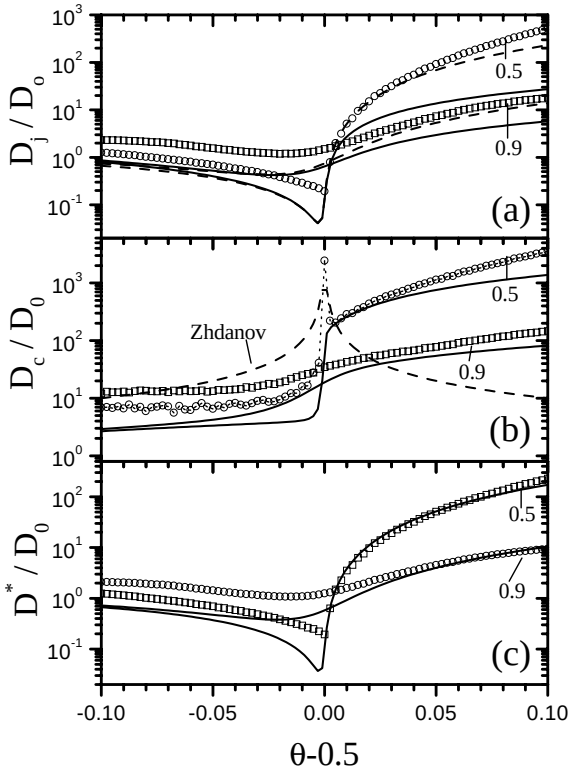

Fig. 2. Normalized jump diffusion coefficient, $D_j/D_\circ$, *vs.* surface coverage θ for two different interaction parameters: $\varphi = 3.53$ (*i.e.* $T = 0.5T_c$) and $\varphi = 1.96$ (*i.e.* $T = 0.9T_c$). The symbols denote MC results. The solid lines represent theoretical results according to equation (22, 23). The dashed lines are calculated using equation (38). (b) Same as (a), but for the normalized chemical diffusion coefficient, $D_c/D_\circ$. The solid lines represent theoretical results calculated from equations (33, 38). (c) Same as (a), but for the normalized tracer diffusion coefficient, $D^*/D_\circ$. The lines represent theoretical results according to equation (39).

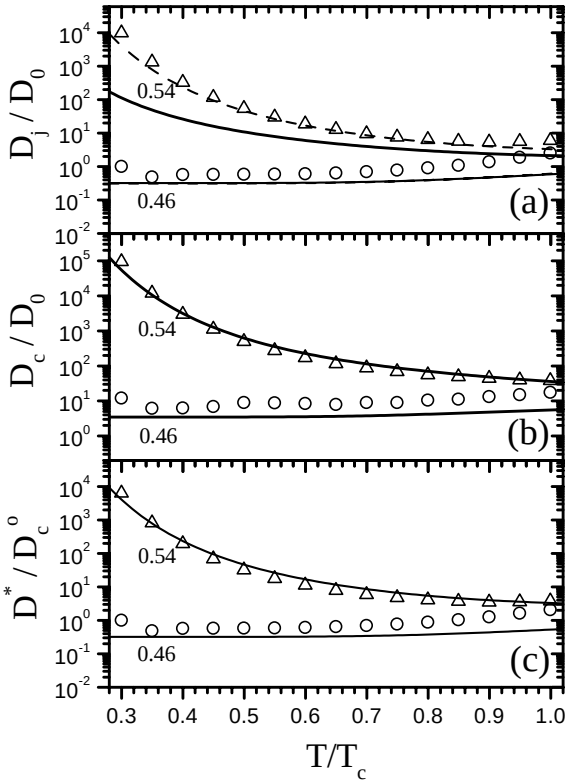

Fig. 3. Temperature dependence of $D_j/D_\circ$ for two different surface coverages θ as indicated on the figure. Temperature is normalized with respect to T_c. The solid (dashed) lines represent theoretical results calculated from equations (22, 23, 38). The symbols denote MC results. (b) Same as (a), but for $D_c/D_\circ$. The lines represent theoretical results calculated from equations (33, 38). (c) Same as (a), but for $D^*/D_\circ$. The lines represent theoretical results according to equation (39).

e.g. [11]). All calculations were carried out in terms of $D_\circ$, the chemical diffusion coefficient for zero interactions between adsorbates on a homogeneous lattice (Langmuir gas) [16].

The mean square number fluctuations $\langle(\delta N)^2\rangle$ determining the thermodynamic factor in the expression for the chemical diffusion coefficient was obtained for a small probe embedded into the whole lattice (for details see [8,16]).

Figure 2a shows the coverage dependence of D_j for two different interaction parameters φ. It is clearly obvious that D_j changes by several orders of magnitude in a narrow range around half coverage at low temperatures ($T = 0.5T_c$), *i.e.* when well-ordered structures are formed. In the close vicinity of half coverage D_j exhibits a deep minimum, which is slightly shifted to coverages $\theta < 0.5$. This finding is in accordance with our analysis in Section 3 and with the results of [12] where also well pronounced minima in the vicinity of stoichiometric concentrations were obtained (see Figs. 9 and 10 of [12]).

Theoretical results obtained according to equations (22, 23) (solid lines), equation (38) (dashed lines) and MC results (symbols) exhibit the same qualitative behavior over a wide range of coverages supporting our main concept of the defect mechanism of adatom transport. The differences between solid and dashed curves emphasize the influence of dimers. Black dimers substantially increase D_j at coverages $\theta > 0.5$, while white dimers slightly decrease D_j at $\theta < 0.5$. The agreement between MC and theory is not quantitative. The best agreement is established at coverages above half coverage, when the dimer motion is taken into account (Eq. (38), dashed lines).

It is probably important to note that the agreement between MC results and theoretical results is better at low temperatures. Close to T_c the defect system cannot be rigorously treated in the frame of a rarefied gas model which was employed in the previous sections and, therefore, the theory can not give a good accuracy here.

The temperature dependence of $D_j/D_\circ$ is shown in Figure 3a for two characteristic surface coverages θ. As already mentioned the best agreement between theory and MC simulation is established at coverages $\theta > 0.5$ when the motion of black dimers is considered (dashed line)

according to equation (38). At $\theta < 0.5$ the deviations between theory and MC are more pronounced, but tend to disappear upon lowering the temperature.

Our results for the chemical diffusion coefficient $D_c = (\partial\mu/\partial \ln\theta) D_j$ are shown in Figure 2b for the same set of interaction parameters. Here we use D_j determined by equation (38), and the thermodynamic factor $\partial\mu/\partial \ln\theta$ determined by equation (33). According to the theory, D_c is a monotonous function of $\delta = \theta - 0.5$, which exhibits substantial increases around half coverage. The transition from white (low mobile) to black (high-mobile) defect transport is responsible for this steep increase.

One can anticipate that relative contributions of different species will be changed with varying the model of the adatom jumps. In a hypothetical case of equal mobilities of black and white defects, no steep behavior of D_c will take place in the vicinity of half coverage. Our idealized model of adatom jumps ignores the very important effect of adatom-adatom interactions in the saddle point. The simplest generalization of this model [11] takes into account the influence of occupied sites in the close vicinity of the saddle point on the jump probabilities of diffusing adatoms. In our case, this interaction will reduce the difference between black and white defect mobilities and the overall diffusion rates as well.

The theoretical results qualitatively agree with the MC data. However, the MC data exhibit a striking maximum of D_c which is clearly visible at $T = 0.5T_c$ and $\delta = 0$, *i.e.* when the adatom layer is almost perfectly ordered. In [11] a similar maximum is explained by a sharp maximum of the thermodynamic factor. Apart from this point there are several minor deviations between MC and theoretical results: (i) for $\delta \to -0.1$ the theoretical results are significantly lower than the MC results (by a factor of 4 at $T = 0.9T_c$), and (ii) for $\delta \to 0.1$ the theoretical results are also lower than the MC results (by a factor of 2 at $T = 0.5T_c$). The theory of adatom diffusion which employs the conception of uncorrelated adatom jumps was developed by Zhdanov in [17]. With this approach one can easily obtain the value of chemical diffusion coefficient as

$$D_c \sim (\delta^2 + e^{-4\varphi})^{-1/2} \tag{44}$$

in the vicinity of $\theta = 0.5$. Equation (44) is shown in Figure 2b as dashed line. It is quite obvious that Zhdanov's theory is capable to explain the maximum in the coverage dependence of D_c at half coverage. However, Zhdanov's approach exhibits significant deviations in the description of D_c at $\delta > 0$.

In Figure 3b the temperature dependence of D_c is shown for two different surface coverages $\theta = 0.46$ and $\theta = 0.54$. For $\theta = 0.54$ the agreement between our theory and MC data is almost quantitative, while for $\theta = 0.46$ there are small deviations which are substantially reduced as the temperature is lowered (similar to the case of D_j).

Figure 2c illustrates the coverage dependencies of the tracer diffusion coefficient, which exhibits a deep minimum at low temperatures (*i.e.* for $T = 0.5T_c$). This minimum was also obtained in [8] (see Figures 7 and 8 of [8]). The coverage dependence $D^*(\theta)$ resembles that of $D_j(\theta)$ (Fig. 2a) and can be discussed in the similar manner as before. There is at least qualitative agreement between MC data and theoretical results calculated from equation (39) for a wide range of coverages $0.4 < \theta < 0.6$. For $\theta > 0.5$ the agreement is almost quantitative, especially at low temperatures. The temperature dependence of D^* shown in Figure 3c clearly demonstrates the excellent agreement between theory (Eq. (39)) and MC results for $\theta = 0.54$, where the motion of black defects and dimers dominate. For $\theta = 0.46$ the agreement between theory and MC is good, especially at low temperatures.

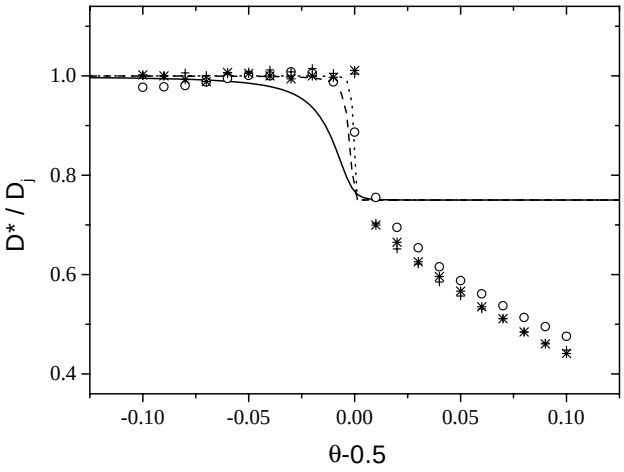

Fig. 4. Coverage dependence of D^*/D_j for various values of the interaction parameter: (1) $\varphi = 2.52$ ($T = 0.7T_c$), solid line: theory, ($\circ$): MC data; (2) $\varphi = 3.53$ ($T = 0.5T_c$), dashed line: theory, ($+$): MC data; (3) $\varphi = 4.41$ ($T = 0.4T_c$), dotted line: theory, ($*$): MC data. The theoretical results are calculated according to equations (38, 39).

It is quite interesting to analyze the behavior of D^*/D_j (Fig. 4). It clearly shows the changes of the transport mechanisms in the coverage range $0.4 < \theta < 0.6$. The flat parts of the curves represent the transport of white defects which prevails at $\theta < 0.5$. Well below half coverage MC and theoretical results (calculated from Eqs. (38, 39)) agree almost quantitatively. A steep decrease from 1 to 3/4 in the vicinity of $\theta = 0.5$ is due to the change of the dominating defect (white defects at $\theta < 0.5$, black defects at $\theta > 0.5$). It should be noted that obtained in [12] nontrivial peculiarities of the relation D^*/D_j were explained in terms of the different transport mechanisms too.

For $\theta > 0.5$ the theory predicts D^*/D_j to be constant. However, the MC results do not support this prediction and exhibit a further decrease of D^*/D_j. It is conceivable that this finding is due to contributions of more complex adatom jumps.

It should be noted that the quantity D^*/D_j was analyzed for the non-interacting case ($\varphi = 0$) by Nakazato and Kitahara and was found to be close to 3/4 at $\theta = 0.5$ [18]. In addition, these authors found a linear dependence of D^*/D_j on θ, in contrast to the present theory. The value D^*/D_j was shown to be higher for a three-dimensional lattice. Our derivation of equation (39) also reveals the

effect of defects jump trajectories. Hence, one can anticipate that D^*/D_j differs for surfaces with various symmetries.

7 Summary

Chemical, jump and tracer diffusion coefficients of repulsively interacting adparticles on a square two-dimensional lattice strongly depend on coverage in the close vicinity of half coverage, where a well-ordered c(2×2) structure is formed at low temperatures. In this work we provide a simple analytical description of an adsorbate system with strong repulsive interaction just for this highly ordered state. Equations for the various diffusion coefficients are obtained explicitly. The comparison of theoretical results and MC simulation data shows good agreement of both approaches for a wide range of coverages $0.4 < \theta < 0.6$ and temperatures, $0.3T_c < T < T_c$.

Our theory employs the concept of the defect motion. It takes into account the adatom jump correlations only in terms of the jump frequency renormalization. The theory can be extended to the cases of other lattice symmetries and greater adatom-adatom interaction radii.

The following points are established.

(i) At an early stage of relaxation, two independent diffusion flows (flows of two defect species) occur with very different diffusion coefficients. As the characteristic length of inhomogeneities increases, the GR processes must be considered. The GR-controlled defect motion produces a locally equilibrium state of the system. Only the last stage of the relaxation is governed by the ordinary diffusion equation with the chemical diffusion coefficient defined by $D_c = (\partial\mu/\partial \ln\theta)D_j$. The independent analysis of defect flows in an external uniform field shows that the jump diffusion coefficient D_j corresponds to the adatom mobility.

(ii) The chemical diffusion coefficient D_c is a monotonous function with very steep behavior near $\theta = 0.5$. This behavior results from the change of the transport mechanism (dominance of white defects at $\theta < 0.5$ and black defects at $\theta > 0.5$).

(iii) D_j and D^* exhibit deep minima in the vicinity of half coverage. These findings are also attributable to the change of the transport mechanism.

(iv) We have explained the difference between the jump and tracer diffusion coefficients appearing for $\theta > 0.5$ where the motion of individual black defects and black dimers prevail. The explanation is based on microscopic jump mechanisms of isolated defects and dimers.

The authors would like to acknowledge stimulating discussions with P. Argyrakis, F. Nieto, A.A. Tarasenko and V. Vikhrenko. This work was financially supported by the Ukrainian State Fund of Fundamental Research (Project #2.4/558) and by the International Association for the promotion of cooperation with scientists from the New Independent States of the former Soviet Union INTAS (#96-0533).

Appendix A: Rate of defect generation

We will use again Figure 1 to illustrate the characteristic three successive steps of pair generation. Let us obtain the probability of pair creation (white defect in site i and black defect in site l on the originally ordered area of the lattice for a short time interval.

(i) The first jump from the site i to site j (jump with the probability $\nu_\circ$ for unit time).

(ii) The lifetime of the adatom in the site j is of the order of $(\nu_\circ e^{3\varphi})^{-1}$ as there are three nearest neighbors. During that time, the adatom at site k can jump to site l with the probability $\nu_\circ e^{\varphi}(\nu_\circ e^{3\varphi})^{-1} = e^{-2\varphi}$.

(iii) The lifetime of the adatom in site l is of order of $(\nu_\circ e^{3\varphi})^{-1}$. During this time, the adatom at site j can jump to site k with the probability $\nu_\circ e^{2\varphi}(\nu_\circ e^{3\varphi})^{-1} = e^{-\varphi}$. This last jump completes the pair generation.

One can see that the total probability of pair creation (a black defect at site l and a white defect at site i) for a short time interval $\Delta t(\nu_\circ \ll \Delta t^{-1} \ll \nu_\circ e^{3\varphi})$ is equal to $\Delta t \nu_\circ e^{-3\varphi}$. We do not describe in details other possibilities of pair generation here. Each of these gives a similar contribution (in the order of magnitude) to the total probability. A simple geometric analysis gives the total probability of pair creation (white defect in site i and black defect in arbitrary site) equal to $G = 28\nu_\circ e^{-3\varphi}$. We can see that the pair generation probability is much lower than the defect jump probability (by the factor of $e^{-(3 or 4)\varphi}$), and this is the reason which allows to treat the defects as an almost ideal gas.

Appendix B: Contribution of black dimers to the total adatom transport

In order to consider the effect of dimers on the jump diffusion coefficient D_j, we employ a technique similar to the one already used in Section 3. We analyze the defect motion in an uniform external field E and consider the contribution of differently oriented dimers on the total adatom flow. For this purpose we have to distinguish the following situations:

a) the black dimer is formed by NN defects in the sites 0 and 5,
   - the probability of the black defect jump $0 \to 6$ for a unit time is equal to $(1/3)\nu_\circ e^{2\varphi}(1 + Ea)$,
   - the probability of the black defect jump $5 \to 6$ is equal to $(1/3)\nu_\circ e^{2\varphi}(1 + Ea/2)$,
   - the probability of the black defect jump $0 \to 7$ is equal to $(1/3)\nu_\circ e^{2\varphi}(1 + Ea/3)$;

b) the black dimer is formed by NNN defects in the sites 0 and 6,
   - the probabilities of $0 \to 5$ and $0 \to 7$ jumps are equal, the value is given by $(1/3)\nu_\circ e^{2\varphi}(1 + Ea/2)$;

c) the black dimer is formed by NNN defects in the sites 5 and 7,
   - the probabilities of $5 \to 6$ and $7 \to 6$ jumps are equal, the value is given by $(1/3)\nu_\circ e^{2\varphi}(1 + 2Ea/3)$.

In the case of the $0 \rightarrow 6$ defect jump, two adatoms are displaced in the positive direction of the field to the distance a, while in the other cases only one adatom is displaced in this direction. The jump probabilities discussed above allow to obtain the contribution of black dimers to the jump diffusion coefficient, ΔD_{j}, which is given by equation (36).

References

1. R. Gomer, Rep. Prog. Phys. **53**, 917 (1990).
2. M. Bowker, D.A. King, Surf. Sci. **71**, 583 (1978).
3. A.A. Chumak, A.A. Tarasenko, Surf. Sci. **91**, 694 (1980).
4. A.A.Tarasenko, A.A. Chumak, Fiz. Tverd. Tela (Leningrad) **22**, 2939 (1980), [Sov. Phys. Solid State **22**, 1716 (1980)].
5. A.A.Tarasenko, A.A. Chumak, Fiz. Tverd. Tela (Leningrad) **24**, 2972 (1982), [Sov. Phys. Solid State **24**, 1683 (1982)].
6. A.A. Tarasenko, A.A. Chumak, Poverkhnost' Fiyika, Khimija, Mekhanika **11**, 98 (1989) (*in Russian*).
7. A.A. Tarasenko, A.A. Chumak, Poverkhnost' Fiyika, Khimija, Mekhanika **12**, 37 (1991) (*in Russian*).
8. C. Uebing, R. Gomer, J. Chem. Phys. **95**, 7626, 7636, 7641, 7648 (1991).
9. Equation (1) is strictly valid only if site exclusion is considered, *i.e.* $n = 0, 1$ for every given lattice site. Double occupancy of sites is forbidden.
10. L. Onsager, Phys. Rev. **65**, 117 (1944).
11. C. Uebing, R. Gomer, Surf. Sci. **381**, 33 (1997).
12. R. Kutner, K. Binder, K.W. Kehr, Phys. Rev. B **28**, 1846 (1983).
13. A. Sadiq, K. Binder, Surf. Sci. **128**, 350 (1983).
14. A.A. Chumak, C. Uebing, Ukrainskij Fizychnij Zhurnal (in print).
15. D.A. Reed, G. Ehrlich, Surf. Sci. **105**, 603 (1981).
16. M. Tringides, R. Gomer, Surf. Sci. **145**, 121 (1984).
17. V.P. Zhdanov, Surf. Sci. Lett. **149**, L13 (1985).
18. K. Nakazato, K. Kitahara, Progr. Theor. Phys. **64**, 2261 (1980).